

Intelligent Reflecting Surface Backscatter Enabled Uplink Coordinated Multi-Cell MIMO Network

Sai Xu, *Member, IEEE*, Chen Chen, *Member, IEEE*, Yanan Du, *Member, IEEE*,
Jiangzhou Wang, *Fellow, IEEE*, and Jie Zhang, *Senior Member, IEEE*

Abstract—This paper proposes an intelligent reflecting surface (IRS) backscatter based uplink coordinated transmission strategy for a radio cellular network, where IRS serves as a transmitter enabling uplink transmission from each user to the associated base station (BS). To be specific, the considered network is made up of multiple cells, each of which consists of one multi-antenna BS and its served users. While one multi-antenna power beacon (PB) is deployed to radiate energy-bearing electromagnetic wave, the radio signal received by each IRS is modulated to send its connective user's information to the associated BS. Based on such a network framework, this paper aims to maximize the weighted sum rate (WSR) under the constraints of total transmit power and reflecting coefficient by joint optimization of active beamforming at the PB, passive beamforming at the IRSs and uplink user scheduling. To address this challenging problem, fractional programming (FP), alternative optimization and weighted bipartite matching are employed to convert the logarithm objective function into a more tractable form and to handle the optimization variables. The simulation results demonstrate the achievable WSR of the considered network.

Index Terms—Intelligent reflecting surface, reconfigurable intelligent surface, backscatter, uplink transmission, fractional programming, alternative optimization, weighted bipartite matching.

I. INTRODUCTION

IN order to support an increasing number of user equipments (UEs), more and more base stations (BSs) are deployed in cellular systems [1]. Accompanied by highly dense BSs and UEs, excessive energy consumption for downlink and uplink wireless communications is caused. For the alleviation of this problem, green communications are always an active research area [2]. As a fully validated wireless technology, multiple-input multiple-output (MIMO), thanks to high degree of freedom resulting from spatial multiplexing, contributes to great improvement of energy efficiency (EE) [3]. Incorporating MIMO into cellular systems, the network capacity is raised

drastically with high spectrum efficiency (SE) and EE. Additionally, multi-cell cooperation is often employed to effectively suppress co-channel interferences among multiple adjacent cells, thereby further facilitating EE [4], [5]. Although coordinated multi-cell MIMO has achieved considerable success, it is still not enough in reducing huge energy consumption of downlink and uplink transmissions between BSs and UEs, and how to implement fundamental improvement remains challenging.

Recently, intelligent reflecting surface (IRS) backscatter as an emerging paradigm has aroused rapidly growing interest, because of its ability to work as a low-power passive transmitter [6], [7]. Typically, IRS is a two-dimensional three-layer programmable metasurface, which consists of a control circuit board inside, a copper plate in the middle and a dielectric substrate outside [8]. On the substrate, a large number of low-cost passive reflecting elements are printed. When the incident signal reaches at each element, its electromagnetic (EM) characteristics, such as amplitude, phase, etc., can be changed in a real-time way [9]. Through collaboration, these elements can realize passive beamforming when the signal is reflected. Since no or few radio frequency (RF) chains are equipped, the power consumption of IRS is generally very low, compared to active antennas [10] and large intelligent surface (LIS) [11]. Therefore, IRS is positioned as an energy-effective enabler to promote wireless communications. On the other hand, backscatter is a technology, with which a device can remodulate the incoming signal to send its own data. During backscatter communications, the device does not transmit any RF signal. Instead, the incoming signal from other transmitters or wireless environment is harnessed to realize information transmission. Clearly, the energy consumption of communications at the device is eliminated by using the backscatter technology. As an integration of IRS and backscatter, IRS backscatter can reap the merits of the two techniques, thus mimicking transmit antennas in a passive way¹.

In this work, we will focus on the IRS backscatter based uplink coordinated transmission strategy for a radio cellular network, while the downlink counterpart has been published in [12]. In this work, UEs in the network are considered to be immobile low-power Internet-of-Things (IoT) devices, each of which is linked to one IRS serving as a passive transmitter to enable uplink transmission. During uplink transmission, a

This work was supported in part by the National Natural Science Foundation of China (62101448); in part by Project funded by the China Postdoctoral Science Foundation (2022M722605); in part by European Commission's Horizon 2020 MSCA Individual Fellowship SICIS under Grant (101032170). (Corresponding author: Yanan Du)

Sai Xu (e-mail: s.xu@sheffield.ac.uk) and Jie Zhang (e-mail: jie.zhang@sheffield.ac.uk) are with the Department of Electronic and Electrical Engineering, University of Sheffield, Sheffield, S10 2TN, UK. Chen Chen (e-mail: C.Chen77@liverpool.ac.uk) is with the Department of Electrical Engineering and Electronics, the University of Liverpool, Liverpool, L69 3GJ, UK. Yanan Du (e-mail: duyanan@nwpu.edu.cn) is with the School of Cybersecurity, Northwestern Polytechnical University, Xi'an, Shaanxi, 710072, China. Jiangzhou Wang (e-mail: j.z.wang@kent.ac.uk) is with the School of Engineering and Digital Arts, University of Kent, Canterbury, CT2 7NT, UK.

Manuscript received XX XX, XXXX; revised XX XX, XXXX.

¹For the paradigm of IRS backscatter, IRS works as a passive transmitter to send its own information by modulating incident signal, which is distinguished from the familiar IRS reflection.

dedicatedly-deployed power beacon (PB) is used to supply signal carrier for information modulation at each IRS, by radiating energy-bearing EM wave. Therefore, a UE is capable of sending its own information to the associated BS via IRS backscatter when scheduled for uplink transmission. Compared to conventional active antennas, the proposed network framework consumes lower transmit power at the UEs and has a lower hardware cost [8].

A. Related Work

Extensive literatures have investigated coordinated multi-cell network, where multi-cell MIMO is one of the most popular research directions. To be specific, Shen *et al.* investigated downlink and uplink communications and proposed a fractional program approach to maximize the weighted sum rate (WSR) of network in [13] and [14]. Choi *et al.* [15] presented a new optimization framework to jointly optimize user selection, power allocation, and precoding in multi-cell multi-user MIMO systems under imperfect CSI at the transmitter. Wu *et al.* [16] studied secure transmission of time-division duplex multi-cell massive MIMO systems under pilot contamination attack with active eavesdropping. In recent years, learning methods have been investigated in IRS-aided wireless communications [17]–[20], including multi-cell network [21], [22]. Balevi *et al.* [21] proposed a deep learning method to acquire channel state information (CSI) for multi-cell interference-limited massive MIMO network. Khan *et al.* [22] employed deep reinforcement learning to maximize the sum-rate in downlink multi-cell network.

In multi-cell network, there exist a few works involving IRS or backscatter techniques. Qiu *et al.* [23] studied IRS-aided multi-cell MISO system, aiming to maximize the sum rate and the minimum signal-to-interference-plus-noise ratio (SINR) among all UEs by jointly optimizing the transmit and reflective beamformers. Xie *et al.* [24] investigated an IRS-aided multi-cell MISO system and maximized the minimum weighted SINR at the UEs. Pan *et al.* [25] investigated the maximization problem of WSR in IRS-aided multi-cell network. Ni *et al.* [26] studied IRS-aided non-orthogonal multiple access (NOMA) techniques in multi-cell network, and maximized the achievable sum rate. Zhang *et al.* [27] investigated an intelligent omni-surface (IOS), which is capable of enabling simultaneous signal reflection and transmission. The authors considered an IOS aided indoor communication scenario, in which an IOS was placed on a wall between two access points (APs). Khan *et al.* [28] and Alevizos *et al.* [29] studied backscatter techniques in multi-cell NOMA network and resource allocation for backscatter enabled multi-cell sensor network, respectively.

Up to now, IRS and backscatter have been separately studied in multi-cell network while IRS backscatter has been underdeveloped. By integrating backscatter techniques, IRS can work as a passive transmitter to send its own information without RF signal transmitting power [30]. As an emerging research area, related works can be found in some literatures, involving signal modulation, cognitive radio system, physical layer security, device-to-device, edge computing, etc. To be

specific, 8-phase shift keying (8PSK) and amplitude-and-phase-varying modulations were investigated in [31] and [32], respectively. Additionally, the hardware implementation was also discussed and analyzed. Dai *et al.* [33] presented a new way for multi-modulation at IRS and realized synthesization of arbitrary constellation diagrams successfully. Considering some practical factors, the optimality of the achievable rate was analyzed asymptotically for an IRS-aided downlink communication system in [34]. Zhao *et al.* [35] discussed whether the backscatter channel or the direct one was stronger in an IRS backscatter communication system. Guan *et al.* [36] considered a cognitive radio system based on IRS backscatter, where the IRS employed backscatter techniques to realize its own information transmission while assisting the primary communication. In our previous work [37], we investigated IRS backscatter and energy harvesting techniques, aiming at offloading computational tasks from network edge to computing servers in a self-sustainable manner. In [38], undesired interference was converted into the desired signal through IRS backscatter techniques. In [39], the confidential transmission was enhanced by changing the confidential signal to artificial noise signal to deteriorate the reception at the eavesdroppers.

B. Contributions of this Paper

Currently, many existing works have demonstrated that it is feasible to employ IRS as a backscatter or transmitter to realize additional transmission, as detailed in the previous subsection. Nevertheless, IRS backscatter coordinated multi-cell network has not been studied except for our published work [12]. This paper will focus on IRS backscatter based uplink coordinated transmission for a radio cellular network, distinguished from downlink communication in [12]. The main contributions of this paper are summarized as follows.

- This paper proposes an IRS backscatter based uplink coordinated transmission framework for a radio cellular network, where IRS serves as a passive transmitter enabling uplink transmission from each UE to the associated BS. During uplink transmission, a dedicated PB is deployed to radiate energy-bearing EM wave, while the radio signal received by each IRS is modulated to send its connective UE's information to the associated BS.
- Based on the established network framework, this paper takes into account the maximization problem of WSR for uplink transmission under the constraints of total transmit power and reflecting coefficient. To address this challenging problem, fractional programming (FP), alternative optimization and weighted bipartite matching are employed to convert the logarithm objective functions into a more tractable form and to handle the optimization variables. Then, active beamforming at the PB, passive beamforming at the IRSs and uplink user scheduling are jointly optimized.
- Extensive simulations are executed to show the relationship between the achievable WSR of system and some important parameters, including the element number of IRS, the total transmit power at the PB, the antenna number of the BSs, the cell number, and the UE number

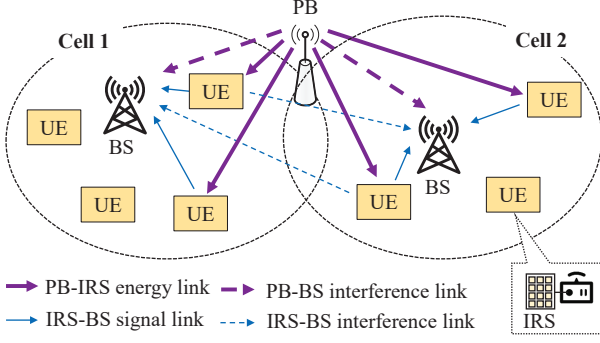


Fig. 1. An illustration of IRS backscatter based uplink coordinated multi-cell MIMO network model.

of each cell. In addition, the robustness of the proposed optimization scheme is simulated and discussed. These results confirm the feasibility of the proposed IRS backscatter based uplink coordinated transmission strategy.

C. Organization

The remainder of this paper is presented as follows. In Section II, the proposed system framework is modelled and the WSR maximization optimization problem is formulated. Section III provides the solving scheme of the optimization problem. Moreover, the complexity is also analyzed. Section IV investigates discrete passive beamforming and analyzes the robustness of the proposed scheme. Simulations are executed in Section V. Section VI draws the conclusions of this paper.

II. SYSTEM MODEL AND PROBLEM FORMULATION

A. System Model

Consider an IRS backscatter based uplink coordinated multi-cell MIMO network, as illustrated in Fig. 1. In such a network, each cell consists of one BS and multiple UEs served by it. Each UE is linked to one IRS, thereby being capable of sending its own information to the associated BS via IRS backscatter when scheduled for uplink transmission. During uplink transmission, a dedicatedly-deployed PB is used to supply signal carrier for information modulation at each IRS, by radiating energy-bearing EM wave. In this network, IRS acts as a passive transmitter instead of a typical signal reflection device. It is assumed that all involved channels remain the same during any one of considered time blocks of interest, but may change over different ones. Other assumptions are that CSI is perfectly acquired for all transmission links², and that the channel and control information is available to the PB, the BSs and all the UEs. Noting that perfect CSI is a strong assumption, the results obtained by the proposed scheme represent the performance upper bound and its robustness with imperfect CSI will be discussed in Section IV-B.

In this network, the notations $\mathcal{I} = \{1, 2, \dots, I\}$ and

$\mathcal{K}_i = \{1, 2, \dots, K_i\}$ are used to denote the sets of BSs (or cells) and UEs served by the i -th BS, respectively. Assume that all BSs and all IRSs have uniform hardware configuration, where each BS is equipped with N antennas and each IRS has L elements with the element set denoted by $\mathcal{L} = \{1, 2, \dots, L\}$. In a time slot, each cell can support up to N UEs for simultaneous uplink transmission, owing to spatial multiplexing brought by multiple antennas. For the i -th cell, the variable $s_{in} \in \mathcal{K}_i$ is introduced to represent the index of the UE who is scheduled in the n -th stream at its BS. Additionally, the PB equipped with M antennas serves the scheduled UEs for their IRS backscatter. Note that if a UE is not scheduled to communicate with its associated BS, its linked IRS is turned into the completely absorbing mode, thereby generating no interference with the BSs.

Let $\mathbf{H}_{s_{in}} \in \mathbb{C}^{L \times M}$, $\mathbf{F}_{j,s_{in}} \in \mathbb{C}^{N \times L}$ and $\mathbf{G}_j \in \mathbb{C}^{N \times M}$ denote the channel gain matrices from the PB to the s_{in} -th UE, from the s_{in} -th UE to the j -th BS, and from the PB to the j -th BS, respectively. When the PB emits EM wave towards scheduled UEs in a time slot, the energy-bearing signal arriving at the IRS is recast to carry new data through modulation. Mathematically, the modulation process at the s_{in} -th IRS, if the corresponding UE is scheduled, is given by

$$\mathbf{F}_{j,s_{in}} \Theta_{s_{in}} \mathbf{H}_{s_{in}} \mathbf{w} s = \mathbf{T}_{j,s_{in}} \theta_{s_{in}} s \xrightarrow{\text{modulate}} \mathbf{T}_{j,s_{in}} \mathbf{v}_{s_{in}} x_{s_{in}},$$

where s and $x_{s_{in}}$ denote the original data from the PB and the modulated data from the s_{in} -th user, with $|s|^2 = 1$ and $\mathbb{E}[|x_{s_{in}}|^2] = 1$, respectively³. The vector \mathbf{w} represents the beamformer at the PB. $\theta_{s_{in}}$ denotes the beamforming vector for the signal s . It is easy to find that $\mathbf{T}_{j,s_{in}} \triangleq \mathbf{F}_{j,s_{in}} \text{diag}\{\mathbf{H}_{s_{in}} \mathbf{w}\}$ and $\Theta_{s_{in}} \triangleq \text{diag}\{\theta_{s_{in}}\}$. From $\theta_{s_{in}} s$ to $\mathbf{v}_{s_{in}} x_{s_{in}}$, the signal modulation at IRS is fulfilled and $\mathbf{v}_{s_{in}}$ can be viewed as the passive beamforming vector for the signal $x_{s_{in}}$. Hence, $[\mathbf{v}_{s_{in}} \mathbf{v}_{s_{in}}^H]_{l,l} \leq 1$ holds, considering that the element reflection coefficient at IRS is not more than one, where $[\cdot]_{l,l}$ denotes the l -th diagonal element of matrix.

Based on this network model, the received signal at the j -th BS is given by

$$\mathbf{y}_j = \sum_{(i,n)} \mathbf{T}_{j,s_{in}} \mathbf{v}_{s_{in}} x_{s_{in}} + \mathbf{G}_j \mathbf{w} s + \mathbf{n}_j,$$

where \mathbf{n}_j is independent and identically distributed (i.i.d.) circularly symmetric complex Gaussian random vector with $\mathbf{n}_j \sim (\mathbf{0}, \sigma^2 \mathbf{I})$. Then, the resulting SINR of the s_{in} -th data stream at the i -th BS is given by

$$\gamma_{i,s_{in}} = \mathbf{v}_{s_{in}}^H \mathbf{T}_{i,s_{in}}^H \left(\sigma^2 \mathbf{I} + \mathbf{G}_i \mathbf{w} \mathbf{w}^H \mathbf{G}_i^H + \sum_{(j,r) \neq (i,n)} \mathbf{T}_{i,s_{jr}} \mathbf{v}_{s_{jr}} \mathbf{v}_{s_{jr}}^H \mathbf{T}_{i,s_{jr}}^H \right)^{-1} \mathbf{T}_{i,s_{in}} \mathbf{v}_{s_{in}}.$$

Thus, the transmission rate from the s_{in} -th UE to the i -th BS

²Channel estimation for IRS-related communication systems is a very challenging task due to the passivity of IRS. How to estimate the channel information for the considered system rapidly and accurately deserves a new thorough contribution beyond this work. Some existing related works such as [40], [41] may help the understanding of channel estimation for the considered system.

³For mathematical tractability, the modulated data symbols are assumed to follow independent identical Gaussian distribution, which is capable of maximizing differential entropy and characterizing the upper bound of communication performance for the considered network.

is given by $R_{i,s_{in}} = \log(1 + \gamma_{i,s_{in}})$.

B. Problem Formulation

Based on the aforementioned model, this paper aims to maximize the WSR of uplink transmission under the constraints of total transmit power and reflecting coefficient by joint optimization of active beamforming at the PB, passive beamforming at the IRSs and uplink user scheduling, which is formulated as⁴

$$\begin{aligned}
 (P0) \quad & \max_{\mathbf{w}, \mathcal{V}, \mathcal{S}} \sum_{(i,n)} \omega_{i,s_{in}} R_{i,s_{in}}, \\
 \text{s.t.} \quad & C1 : \text{Tr}(\mathbf{w}\mathbf{w}^H) \leq P, \\
 & C2 : [\mathbf{v}_{s_{in}} \mathbf{v}_{s_{in}}^H]_{l,l} \leq 1, \quad l \in \mathcal{L} \\
 & C3 : s_{in} \in \mathcal{K}_i \cup \{\emptyset\},
 \end{aligned}$$

where \mathcal{V} and \mathcal{S} refer to the collections of $\mathbf{v}_{s_{in}}$ and s_{in} , respectively. The weighting factor $\omega_{i,s_{in}}$ accounts for the priority of the s_{in} -th UE at the i -th BS. P denotes the allowable maximum transmit power overhead of the PB. Note that the allowable maximum number of scheduled UEs per cell is N , which is bounded by the antenna number of each BS.

III. UPLINK WSR MAXIMIZATION

The problem (P0) is challenging to address directly, since the optimization variables \mathbf{w} , $\mathbf{v}_{s_{in}}$, and s_{in} are deeply coupled and the objective function is in a form of weighted sum of logarithm functions. To handle the problem (P0), this section will firstly employ Lagrangian dual transform, being a typical method of FP, to convert the objective function into a new form. Then, alternative optimization and weighted bipartite matching are adopted to optimize \mathbf{w} , $\mathbf{v}_{s_{in}}$ and s_{in} . Finally, the computational complexity is analyzed.

A. Objective Function Conversion

The objective function of the problem (P0) is in a form of weighted sum of logarithm functions. To make the problem (P0) more tractable, Lagrangian dual transform is leveraged to convert the objective function into a new form. Specifically, introducing auxiliary variable $\alpha_{i,s_{in}}$, the weighted sum of logarithm functions is transformed into

$$\begin{aligned}
 \sum_{(i,n)} \omega_{i,s_{in}} R_{i,s_{in}} &= \sum_{(i,n)} \omega_{i,s_{in}} \log(1 + \gamma_{i,s_{in}}) \\
 &= \max_{\alpha_{i,s_{in}} \geq 0} \sum_{(i,n)} \omega_{i,s_{in}} [\log(1 + \alpha_{i,s_{in}}) - \alpha_{i,s_{in}}] \\
 &\quad + \frac{\omega_{i,s_{in}} (1 + \alpha_{i,s_{in}}) \gamma_{i,s_{in}}}{1 + \gamma_{i,s_{in}}}.
 \end{aligned}$$

⁴In this paper, it is assumed that each reflecting element at the IRS can be individually adjusted. When more sophisticated IRS models, such as the physics-based model and the impedance network-based model [42], are employed, the formulated optimization problem (P0) and its solving scheme need to be adaptively changed.

Using quadratic transform [13], we have

$$\begin{aligned}
 \frac{\omega_{i,s_{in}} (1 + \alpha_{i,s_{in}}) \gamma_{i,s_{in}}}{1 + \gamma_{i,s_{in}}} &= \frac{\omega_{i,s_{in}} (1 + \alpha_{i,s_{in}}) |A_{i,s_{in}}|^2}{B_i} \\
 &= 2\sqrt{\omega_{i,s_{in}} (1 + \alpha_{i,s_{in}})} \text{Re}\{\beta_{i,s_{in}}^H A_{i,s_{in}}\} - \beta_{i,s_{in}}^H B_i \beta_{i,s_{in}},
 \end{aligned}$$

where $\beta_{i,s_{in}}$ is an auxiliary variable vector, and $A_{i,s_{in}}$ and B_i are respectively given by

$$\begin{aligned}
 A_{i,s_{in}} &= \mathbf{T}_{i,s_{in}} \mathbf{v}_{s_{in}}, \\
 B_i &= \sigma^2 \mathbf{I} + \mathbf{G}_i \mathbf{w} \mathbf{w}^H \mathbf{G}_i^H + \sum_{(j,r)} \mathbf{T}_{i,s_{jr}} \mathbf{v}_{s_{jr}} \mathbf{v}_{s_{jr}}^H \mathbf{T}_{i,s_{jr}}^H.
 \end{aligned}$$

Thus, the problem (P0) is reformulated as

$$\begin{aligned}
 (P1) \quad & \max_{\mathbf{w}, \mathcal{V}, \mathcal{S}, \alpha, \beta} f(\mathbf{w}, \mathcal{V}, \mathcal{S}, \alpha, \beta), \\
 & C1 - C3, \\
 & C4 : \alpha_{i,s_{in}} \geq 0,
 \end{aligned}$$

where α and β refer to the collections of $\alpha_{i,s_{in}}$ and $\beta_{i,s_{in}}$, and

$$\begin{aligned}
 f(\mathbf{w}, \mathcal{V}, \mathcal{S}, \alpha, \beta) &\triangleq \sum_{(i,n)} \omega_{i,s_{in}} [\log(1 + \alpha_{i,s_{in}}) - \alpha_{i,s_{in}}] \\
 &\quad + 2\sqrt{\omega_{i,s_{in}} (1 + \alpha_{i,s_{in}})} \text{Re}\{\beta_{i,s_{in}}^H A_{i,s_{in}}\} - \beta_{i,s_{in}}^H B_i \beta_{i,s_{in}}.
 \end{aligned}$$

Since the optimization variables \mathbf{w} , $\mathbf{v}_{s_{in}}$, and s_{in} are deeply coupled in the constraints, the problem (P1) is still challenging to solve directly. In the following subsection, we will present an alternative optimization method to solve the problem (P1).

B. Alternative Optimization

This subsection will provide an alternative optimization procedure to address the problem (P1) by cyclically optimizing the variables α , β , \mathbf{w} , \mathcal{V} and \mathcal{S} , which is divided into three steps.

Step-1): Optimizing α and β

Given \mathbf{w} , \mathcal{V} , and \mathcal{S} , we separately take a derivative with respect to $\alpha_{i,s_{in}}$ and $\beta_{i,s_{in}}$ to obtain the optimal $\alpha_{i,s_{in}}^\circ$ and $\beta_{i,s_{in}}^\circ$. Mathematically, let

$$\begin{aligned}
 \frac{\partial f(\mathbf{w}, \mathcal{V}, \mathcal{S}, \alpha, \beta)}{\partial \alpha_{i,s_{in}}} &= 0, \\
 \frac{\partial f(\mathbf{w}, \mathcal{V}, \mathcal{S}, \alpha, \beta)}{\partial \beta_{i,s_{in}}} &= 0.
 \end{aligned}$$

It is derived that the optimal $\alpha_{i,s_{in}}^\circ$ and $\beta_{i,s_{in}}^\circ$ are respectively given by

$$\begin{aligned}
 \alpha_{i,s_{in}}^\circ &= \gamma_{i,s_{in}}, \\
 \beta_{i,s_{in}}^\circ &= \sqrt{\omega_{i,s_{in}} (1 + \alpha_{i,s_{in}})} B_i^{-1} A_{i,s_{in}}.
 \end{aligned}$$

Step-2): Optimizing \mathbf{w}

With α , β , \mathcal{V} , and \mathcal{S} given, the objective function of the problem (P1) can be simplified as

$$\max_{\mathbf{w}} f(\mathbf{w}, \mathcal{V}, \mathcal{S}, \alpha, \beta)$$

$$\Longleftrightarrow \min_{\mathbf{w}} \sum_{(i,n)} \mathbf{w}^H \mathbf{Y}_{i,s_{in}} \mathbf{w} - 2\text{Re}\{\mathbf{w}^H \mathbf{x}_{i,s_{in}}\},$$

where

$$\begin{aligned} \mathbf{Y}_{i,s_{in}} &= \left[\mathbf{G}_i^H \beta_{i,s_{in}} \beta_{i,s_{in}}^H \mathbf{G}_i + \sum_{(j,r)} (\beta_{i,s_{in}}^H \mathbf{F}_{i,s_{jr}} \boldsymbol{\Theta}_{s_{jr}} \mathbf{H}_{s_{jr}})^H \beta_{i,s_{in}}^H \mathbf{F}_{i,s_{jr}} \boldsymbol{\Theta}_{s_{jr}} \mathbf{H}_{s_{jr}} \right], \\ \mathbf{x}_{i,s_{in}} &= \sqrt{\omega_{i,s_{in}}(1 + \alpha_{i,s_{in}})} (\beta_{i,s_{in}}^H \mathbf{F}_{i,s_{in}} \boldsymbol{\Theta}_{s_{in}} \mathbf{H}_{s_{in}})^H, \end{aligned}$$

To make the problem (P1) tractable, semidefinite relaxation (SDR) is performed to lift (P1) into a higher dimension. Specifically, let $\mathbf{W} = \mathbf{w}\mathbf{w}^H$, $\hat{\mathbf{W}} = \hat{\mathbf{w}}\hat{\mathbf{w}}^H$, and

$$\hat{\mathbf{w}} = \begin{bmatrix} \mathbf{w} \\ 1 \end{bmatrix}, \quad \mathbf{X}_{i,s_{in}} = \begin{bmatrix} \mathbf{0} & \mathbf{x}_{i,s_{in}} \\ \mathbf{x}_{i,s_{in}}^H & 0 \end{bmatrix}.$$

Then, the objective function of the problem (P1) is further given by

$$\begin{aligned} & \max_{\mathbf{w}} f(\mathbf{w}, \mathcal{V}, \mathcal{S}, \alpha, \beta) \\ & \Longleftrightarrow \min_{\mathbf{w}} \sum_{(i,n)} \text{Tr}(\mathbf{Y}_{i,s_{in}} \mathbf{W}) - \text{Tr}(\mathbf{X}_{i,s_{in}} \hat{\mathbf{W}}). \end{aligned}$$

Thus, this problem (P1) is equivalently rewritten as

$$\begin{aligned} \text{(P2)} \quad & \min_{\hat{\mathbf{W}}} \sum_{(i,n)} \text{Tr}(\mathbf{Y}_{i,s_{in}} \mathbf{W}) - \text{Tr}(\mathbf{X}_{i,s_{in}} \hat{\mathbf{W}}), \\ & \text{s.t.} \quad \text{C5} : \text{Tr}(\mathbf{W}) \leq P, \\ & \quad \text{C6} : [\hat{\mathbf{W}}]_{M+1,M+1} = 1, \\ & \quad \text{C7} : \hat{\mathbf{W}} \succeq \mathbf{0}, \\ & \quad \text{C8} : \text{rank}(\hat{\mathbf{W}}) = 1. \end{aligned}$$

Dropping the constraint C8, the problem (P2) is relaxed as a convex semidefinite program (SDP) problem and can be addressed by existing CVX solvers. Then, the rank-one solution \mathbf{w}° can be recovered by using singular value decomposition (SVD) if the rank of the optimal \mathbf{W}° is one. Otherwise, the Gaussian randomization method may be used to recover the rank-one solution \mathbf{w}° or the eigenvector corresponding to the maximum eigenvalue of \mathbf{W}° is approximately used as \mathbf{w}° .

Step-3): Optimizing \mathcal{V} and \mathcal{S}

Given \mathbf{w} , α and β , the objective function of the problem (P1) is simplified as

$$\begin{aligned} & \max_{\mathcal{V}} f(\mathbf{w}, \mathcal{V}, \mathcal{S}, \alpha, \beta) \\ & \Longleftrightarrow \max_{\mathcal{V}} \sum_{(i,n)} 2\sqrt{\omega_{i,s_{in}}(1 + \alpha_{i,s_{in}})} \text{Re}\{\beta_{i,s_{in}}^H \mathbf{A}_{i,s_{in}}\} \\ & \quad - \beta_{i,s_{in}}^H \mathbf{B}_i \beta_{i,s_{in}} \\ & \Longleftrightarrow \max_{\mathcal{V}} \sum_{(i,n)} 2\sqrt{\omega_{i,s_{in}}(1 + \alpha_{i,s_{in}})} \text{Re}\{\beta_{i,s_{in}}^H \mathbf{T}_{i,s_{in}} \mathbf{v}_{s_{in}}\} \\ & \quad - \beta_{i,s_{in}}^H \left(\sum_{(j,r)} \mathbf{T}_{i,s_{jr}} \mathbf{v}_{s_{jr}} \mathbf{v}_{s_{jr}}^H \mathbf{T}_{i,s_{jr}}^H \right) \beta_{i,s_{in}}. \end{aligned}$$

According to quadratic constrained quadratic programming

(QCQP), it is easy to derive that

$$\begin{aligned} 2\text{Re}\{\beta_{i,s_{in}}^H \mathbf{T}_{i,s_{in}} \mathbf{v}_{s_{in}}\} &= \text{Tr}(\boldsymbol{\Omega}_{i,s_{in}} \hat{\mathbf{V}}_{s_{in}}), \\ \beta_{i,s_{in}}^H \left(\mathbf{T}_{i,s_{jr}} \mathbf{v}_{s_{jr}} \mathbf{v}_{s_{jr}}^H \mathbf{T}_{i,s_{jr}}^H \right) \beta_{i,s_{in}} &= \\ & \quad \text{Tr} \left(\beta_{i,s_{in}} \beta_{i,s_{in}}^H \mathbf{T}_{i,s_{jr}} \mathbf{V}_{s_{jr}} \mathbf{T}_{i,s_{jr}}^H \right), \end{aligned}$$

where $\mathbf{V}_{s_{jr}} \triangleq \mathbf{v}_{s_{jr}} \mathbf{v}_{s_{jr}}^H$, $\hat{\mathbf{V}}_{s_{in}} \triangleq \hat{\mathbf{v}}_{s_{in}} \hat{\mathbf{v}}_{s_{in}}^H$, and

$$\boldsymbol{\Omega}_{i,s_{in}} = \begin{bmatrix} \mathbf{0} & (\beta_{i,s_{in}}^H \mathbf{T}_{i,s_{in}})^H \\ \beta_{i,s_{in}}^H \mathbf{T}_{i,s_{in}} & 0 \end{bmatrix}, \quad \hat{\mathbf{v}}_{s_{in}} = \begin{bmatrix} \mathbf{v}_{s_{in}} \\ 1 \end{bmatrix}.$$

Based on this, the new objective function is given by

$$\begin{aligned} & \max_{\mathcal{V}} f(\mathbf{w}, \mathcal{V}, \mathcal{S}, \alpha, \beta) \\ & \Longleftrightarrow \max_{\mathcal{V}} \sum_{(i,n)} \left[\sqrt{\omega_{i,s_{in}}(1 + \alpha_{i,s_{in}})} \text{Tr}(\boldsymbol{\Omega}_{i,s_{in}} \hat{\mathbf{V}}_{s_{in}}) \right. \\ & \quad \left. - \sum_{(j,r)} \text{Tr} \left(\beta_{i,s_{in}} \beta_{i,s_{in}}^H \mathbf{T}_{i,s_{jr}} \mathbf{V}_{s_{jr}} \mathbf{T}_{i,s_{jr}}^H \right) \right]. \end{aligned}$$

Thus, the problem (P1) is reformulated as

$$\begin{aligned} \text{(P3)} \quad & \max_{\mathcal{V}} \sum_{(i,n)} \left[\sqrt{\omega_{i,s_{in}}(1 + \alpha_{i,s_{in}})} \text{Tr}(\boldsymbol{\Omega}_{i,s_{in}} \hat{\mathbf{V}}_{s_{in}}) \right. \\ & \quad \left. - \sum_{(j,r)} \text{Tr} \left(\beta_{i,s_{in}} \beta_{i,s_{in}}^H \mathbf{T}_{i,s_{jr}} \mathbf{V}_{s_{jr}} \mathbf{T}_{i,s_{jr}}^H \right) \right], \\ & \text{s.t.} \quad \text{C4} : s_{in} \in \mathcal{K}_i \cup \{\emptyset\}, \\ & \quad \text{C9} : [\hat{\mathbf{V}}_{s_{in}}]_{l,l} \leq 1, \quad l \in \mathcal{L}, \\ & \quad \text{C10} : [\hat{\mathbf{V}}_{s_{in}}]_{L+1,L+1} = 1, \\ & \quad \text{C11} : \hat{\mathbf{V}}_{s_{in}} \succeq \mathbf{0}, \\ & \quad \text{C12} : \text{rank}(\hat{\mathbf{V}}_{s_{in}}) = 1. \end{aligned}$$

If the user scheduling \mathcal{S} is given, the maximum uplink WSR can be acquired by cyclically optimizing α , β , \mathbf{w} , and \mathcal{V} . When the number of cell UEs (i.e. UEs within a cell) is small, the optimal \mathcal{S}° can be obtained by going through all the user scheduling cases. However, when the number of cell UEs is large, the ergodic user scheduling method has an extremely high computational complexity.

To acquire the optimal \mathcal{S}° quickly, weighted bipartite matching is adopted. To be specific, the variable $s_{in} \in \mathcal{K}_i$ represents the index of the UE who is scheduled in the n -th stream at the i -th BS. In this assignment, the maximum uplink transmission rate of the s_{in} -th UE is denoted by $\xi_{s_{in},n}$. By observing the problem (P3), it is not difficult to find that the passive beamforming matrix $\hat{\mathbf{V}}_{s_{in}}$ at the scheduled s_{in} -th UE is independent of the scheduling and passive beamforming in other streams. In other words, the passive beamforming matrix for each cell UE when scheduled to any a stream can be separately optimized, which is given by

$$\text{(P3')} \quad \max_{\mathcal{V}} \sqrt{\omega_{i,s_{in}}(1 + \alpha_{i,s_{in}})} \text{Tr}(\boldsymbol{\Omega}_{i,s_{in}} \hat{\mathbf{V}}_{s_{in}})$$

Algorithm 1 Overall algorithm for the problem (P1)

1: **Initialization:** Set $t = 0$, ε , \mathbf{w} , $\mathbf{v}_{s_{in}}$, $f_{\text{opt}}^{(t)}$.
2: **repeat**
3: Set $t = t + 1$.
4: Compute $\alpha^{(t)}$ and $\beta^{(t)}$.
5: Solve (P2) to obtain $\mathbf{w}^{(t)}$.
6: Jointly optimize (P3') and (P3'') to obtain $\mathcal{V}^{(t)}$ and $\mathcal{S}^{(t)}$.
7: Compute $f_{\text{opt}}^{(t)} = f(\mathbf{w}^{(t)}, \mathcal{V}^{(t)}, \mathcal{S}^{(t)}, \alpha^{(t)}, \beta^{(t)})$.
8: **until** $\frac{f_{\text{opt}}^{(t)} - f_{\text{opt}}^{(t-1)}}{f_{\text{opt}}^{(t)}} < \varepsilon$.
9: **return** $f_{\text{opt}}^{(t)}$.

$$-\sum_{(j,r)} \text{Tr} \left(\beta_{j,s_{jr}} \beta_{j,s_{jr}}^H \mathbf{T}_{j,s_{in}} \mathbf{V}_{s_{in}} \mathbf{T}_{j,s_{in}}^H \right),$$

s.t. C9 ~ C12.

Ignoring the constraint C12, the problem (P3) is convex over $\hat{\mathbf{V}}_{s_{in}}^{\circ}$ and easy to solve. Based on the obtained optimal solution $\hat{\mathbf{V}}_{s_{in}}^{\circ}$, the rank-one solution $\mathbf{v}_{s_{in}}^{\circ}$ can be recovered by using SVD or the Gaussian randomization method. Then, $\xi_{s_{in},n}$ can be computed by

$$\begin{aligned} \xi_{s_{in},n} = & \omega_{i,s_{in}} [\log(1 + \alpha_{i,s_{in}}) - \alpha_{i,s_{in}}] + \sigma^2 \beta_{i,s_{in}}^H \beta_{i,s_{in}} + \\ & \beta_{i,s_{in}}^H \mathbf{G}_i \mathbf{w} \mathbf{w}^H \mathbf{G}_i^H \beta_{i,s_{in}} + \sqrt{\omega_{i,s_{in}} (1 + \alpha_{i,s_{in}})} \text{Tr}(\Omega_{i,s_{in}} \hat{\mathbf{V}}_{s_{in}}) \\ & - \sum_{(j,r)} \text{Tr} \left(\beta_{j,s_{jr}} \beta_{j,s_{jr}}^H \mathbf{T}_{j,s_{in}} \mathbf{V}_{s_{in}} \mathbf{T}_{j,s_{in}}^H \right). \end{aligned}$$

This fact that the passive beamforming matrix for each cell UE when scheduled to any a stream can be separately optimized allows solving \mathcal{V} and \mathcal{S} jointly by weighted bipartite matching. By optimizing the problem (P3'), $\xi_{s_{in},n}$ can be obtained. Then, the problem (P3) for given $\xi_{s_{in},n}$ is simplified as a weighted bipartite matching problem as follows.

$$\begin{aligned} \text{(P3'')} \quad & \max_{\mathcal{V}} \sum_{s_{in} \in \mathcal{K}_i} \sum_{n=1}^N x_{s_{in},n} \xi_{s_{in},n}, \\ \text{s.t.} \quad & \text{C13: } \sum_{s_{in} \in \mathcal{K}_i} x_{s_{in},n} \leq 1, \\ & \text{C14: } \sum_{n=1}^N x_{s_{in},n} \leq 1, \\ & \text{C15: } x_{s_{in},n} \in \{0, 1\}, \end{aligned}$$

where the binary variable $x_{s_{in},n} = 1$ indicates that the s_{in} -th UE is scheduled in the n -th stream at the i -th BS and otherwise $x_{s_{in},n} = 0$. Note that each BS is considered individually in the matching problem (P3'').

C. Computational Complexity Analysis

The problem (P0) is firstly converted into an equivalent problem (P1) by employing Lagrangian dual transform and FP. Then, the problem (P1) is decomposed into three steps for alternative optimization of $\alpha_{i,s_{in}}$, $\beta_{i,s_{in}}$, \mathbf{w} , \mathcal{V} , and \mathcal{S} . The overall algorithm for the problem (P1) is presented in Algorithm 1. Since the objective function varies in the three steps of alternative optimization, Algorithm 1 does not belong to block coordinate ascent. Nevertheless, the iterative process

converges, as specified in Proposition 1.

Proposition 1: Algorithm 1 converges, with the WSR of the considered network monotonically nondecreasing per iteration. The final solution is a stationary point if the user scheduling is given.

Proof: See Appendix B. ■

Compared with the second and third steps, the computational complexity of the first one is negligible because the closed expressions of the optimal $\alpha_{i,s_{in}}^{\circ}$ and $\beta_{i,s_{in}}^{\circ}$ are available. For the second step, its computational complexity depends on the problem (P2). Dropping the rank-one constraint, its computational complexity, using the interior-point method (IPM), is given by

$$C_{p2} = \frac{\sqrt{2M+4}}{\varepsilon} \left[8n_1(M+1)^3 + 4n_1^2(M+1)^2 + 2n_1^2 + 2n_1 \right],$$

where ε denotes the iteration accuracy and $n_1 = \mathcal{O}\{4(M+1)^2\}$. For the third step, its computational complexity depends on the problems (P3') and (P3''). Dropping the rank-one constraint, the computational complexity of the problem (P3') is given by

$$C_{p3'} = \frac{\sqrt{3L+5}}{\varepsilon} \left[8n_2(L+1)^3 + 4n_2^2(L+1)^2 + (n_2^2 + n_2)(L+1) \right],$$

where $n_2 = \mathcal{O}\{4IN(L+1)^2\}$. For the weighted bipartite matching problem (P3''), its computational complexity with finite precision is given by $C_{p3''} = \mathcal{O}\{(K+N)^2\}$ [14]. For the rank-one solution recovery of \mathbf{w} and $\mathbf{v}_{s_{in}}$, the computational complexity is negligibly small. Therefore, the total complexity of the problem (P1) is approximated as

$$C_{p1} = T_{\text{ite}}(C_{p2} + IKC_{p3'} + C_{p3''}),$$

where T_{ite} is the iteration number for the cyclical alternate process.

IV. EXTENSIONS

This section will discuss discrete passive beamforming at IRS and evaluate the robustness of the proposed optimization scheme in the case of imperfect CSI.

A. Discrete Passive Beamforming

Hereinbefore, the passive beamforming $\mathbf{v}_{s_{in}}$ is assumed to be continuously adjustable as long as the constraint $[\mathbf{v}_{s_{in}} \mathbf{v}_{s_{in}}^H]_{l,l} \leq 1$ is satisfied. However, discrete phase and amplitude at IRS is more cost-effective to implement, because of its hardware limitation, than the continuous one [43].⁵ Hence, this subsection considers the discrete passive beamforming $\tilde{\mathbf{v}}_{s_{in}}$, which is restricted to a set of discrete phase and

⁵In IRS-aided communication systems, discrete phase and amplitude configurations, which are different from discrete phase and amplitude, have been investigated in some literatures [42], [44], [45], aiming to reduce the overhead for channel estimation and the complexity of online optimization.

amplitude values at each element of IRS

$$\Psi = \{\phi_1, \phi_2, \dots, \phi_P\}.$$

In this set, each $\phi_p \in \mathbb{C}^{L \times 1}$, $p = 1, 2, \dots, P$, represents a possible passive beamforming vector. To acquire the optimal $\tilde{\mathbf{v}}_{s_{in}}$ from the set quickly, we adopt the method given in [14]. According to [14], the WSR of uplink transmission is firstly maximized and the solution $\mathbf{v}_{s_{in}}$ is obtained by continuously optimizing adjustable phase and amplitude at IRS. Then, a discrete solution $\phi_p \in \Psi$ that is the closest to the solution $\mathbf{v}_{s_{in}}$ is used as the heuristic suboptimal discrete passive beamforming vector $\tilde{\mathbf{v}}_{s_{in}}$. Mathematically, the solution is given by

$$\tilde{\mathbf{v}}_{s_{in}} = \arg \max_{\phi_p \in \Psi} \|\phi_p - \mathbf{v}_{s_{in}}\|_2.$$

Clearly, this problem is easy to address.

B. Robustness under Imperfect CSI

When imperfect CSI is considered, the optimization problem is often formulated as a robust optimization problem [46], which deserves a new thorough investigation. In this subsection, we will only shed light on the robustness of the proposed optimization scheme with imperfect CSI, where the components related to the CSI errors are simply modelled as white Gaussian noises for approximate treatment. To be specific, $\mathbf{H}_{s_{in}}$, $\mathbf{F}_{j,s_{in}}$ and \mathbf{G}_j can be mathematically rewritten as $\mathbf{H}_{s_{in}} = \bar{\mathbf{H}}_{s_{in}} + \tilde{\mathbf{H}}_{s_{in}}$, $\mathbf{F}_{j,s_{in}} = \bar{\mathbf{F}}_{j,s_{in}} + \tilde{\mathbf{F}}_{j,s_{in}}$ and $\mathbf{G}_j = \bar{\mathbf{G}}_j + \tilde{\mathbf{G}}_j$, respectively, where $\bar{\mathbf{H}}_{s_{in}}$, $\bar{\mathbf{F}}_{j,s_{in}}$, $\bar{\mathbf{G}}_j$ and $\tilde{\mathbf{H}}_{s_{in}}$, $\tilde{\mathbf{F}}_{j,s_{in}}$, $\tilde{\mathbf{G}}_j$ are channel estimations and error matrices of $\mathbf{H}_{s_{in}}$, $\mathbf{F}_{j,s_{in}}$ and \mathbf{G}_j . Moreover, each element of $\tilde{\mathbf{H}}_{s_{in}}$, $\tilde{\mathbf{F}}_{j,s_{in}}$, $\tilde{\mathbf{G}}_j$ follows $(0, \rho^2 \Sigma_{\mathbf{H}_{s_{in}}})$, $(0, \rho^2 \Sigma_{\mathbf{F}_{j,s_{in}}})$ and $(0, \rho^2 \Sigma_{\mathbf{G}_j})$, respectively. Based on this channel model, it can be deduced that

$$\begin{aligned} \mathbf{G}_j \mathbf{w} &= \bar{\mathbf{G}}_j \mathbf{w} + \tilde{\mathbf{G}}_j \mathbf{w}, \\ \mathbf{T}_{j,s_{in}} &= \bar{\mathbf{T}}_{j,s_{in}} + \tilde{\mathbf{T}}_{j,s_{in}}, \\ \bar{\mathbf{T}}_{j,s_{in}} &= \bar{\mathbf{F}}_{j,s_{in}} \text{diag}\{\bar{\mathbf{H}}_{s_{in}} \mathbf{w}\}, \\ \tilde{\mathbf{T}}_{j,s_{in}} &\approx \tilde{\mathbf{F}}_{j,s_{in}} \text{diag}\{\bar{\mathbf{H}}_{s_{in}} \mathbf{w}\} + \bar{\mathbf{F}}_{j,s_{in}} \text{diag}\{\tilde{\mathbf{H}}_{s_{in}} \mathbf{w}\}. \end{aligned}$$

Since it is assumed that the components related to the CSI errors can be modelled as white Gaussian noises, $\bar{\mathbf{F}}_{j,s_{in}} \text{diag}\{\tilde{\mathbf{H}}_{s_{in}} \mathbf{w}\} \mathbf{v}_{s_{in}} \sim \mathcal{CN}(\mathbf{0}, \Omega_{j,s_{in}, \mathbf{H}_{s_{in}}})$ can be deduced with the diagonal elements of $\Omega_{j,s_{in}, \mathbf{H}_{s_{in}}}$ being $\rho^2 P \Sigma_{\mathbf{H}_{s_{in}}} \|\mathbf{f}_{j,s_{in}}^{(m)}\|^2$ and other elements being approximated as zero. $\mathbf{f}_{j,s_{in}}^{(m)}$ represents the m -th row vector of $\bar{\mathbf{F}}_{j,s_{in}}$. For $\tilde{\mathbf{F}}_{j,s_{in}} \text{diag}\{\bar{\mathbf{H}}_{s_{in}} \mathbf{w}\} \mathbf{v}_{s_{in}}$, it approximatively obeys the distribution $\tilde{\mathbf{F}}_{j,s_{in}} \text{diag}\{\bar{\mathbf{H}}_{s_{in}} \mathbf{w}\} \mathbf{v}_{s_{in}} \sim \mathcal{CN}(\mathbf{0}, \Omega_{j,s_{in}, \mathbf{F}_{j,s_{in}}})$ with the diagonal elements of $\Omega_{j,s_{in}, \mathbf{F}_{j,s_{in}}}$ being $\frac{\rho^2 P \Sigma_{\mathbf{F}_{j,s_{in}}} \|\bar{\mathbf{H}}_{s_{in}}\|^2}{M}$ and other elements being approximated as zero. Additionally, $\tilde{\mathbf{G}}_j \mathbf{w} \sim (0, \Omega_{\mathbf{G}_j})$, where $\Omega_{\mathbf{G}_j} = \rho^2 P \Sigma_{\mathbf{F}_{j,s_{in}}}$. Therefore, the resulting SINR of the s_{in} -th data stream at the i -th BS is given by

$$\gamma_{i,s_{in}} \approx \mathbf{v}_{s_{in}}^H \bar{\mathbf{T}}_{i,s_{in}}^H \left(\Sigma + \bar{\mathbf{G}}_i \mathbf{w} \mathbf{w}^H \bar{\mathbf{G}}_i^H \right)^{-1} \bar{\mathbf{T}}_{i,s_{in}} \mathbf{v}_{s_{in}},$$

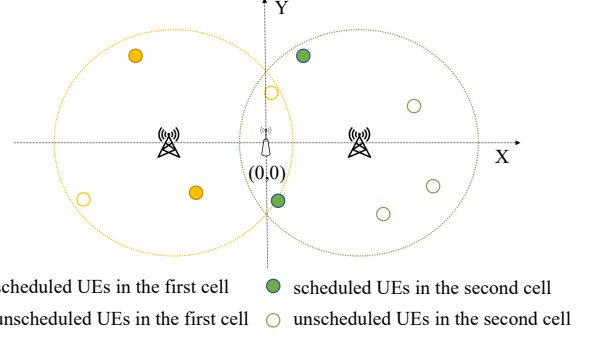


Fig. 2. Spatial distribution of PB, BSs and UEs.

TABLE I
SIMULATION PARAMETERS.

Notation	Description	Value
κ	Rician factor	3
d_0	Reference distance	1m
d	Distances from PB to BSs	50 m
r	Cell radius	60 m
I	Cell or BS number	2
K	UE number in single cell	2
M	Antenna number of PB	4
N	Antenna number of BSs	2
L	Element number of IRS	64
P	Total transmit power of PB	9 dBW
P_a	Transmit power of each active UE	3 dBm
σ^2	Noise variance	-94 dBm
ω_{jk}	Weighting factor	1

$$+ \sum_{(j,r) \neq (i,n)} \bar{\mathbf{T}}_{i,s_{jr}} \mathbf{v}_{s_{jr}} \mathbf{v}_{s_{jr}}^H \bar{\mathbf{T}}_{i,s_{jr}}^H \Big)^{-1} \bar{\mathbf{T}}_{i,s_{in}} \mathbf{v}_{s_{in}},$$

where

$$\Sigma \approx \sigma^2 \mathbf{I} + \Omega_{\mathbf{G}_j} + \sum_{(j,r)} \Omega_{j,s_{in}, \mathbf{H}_{s_{in}}} + \sum_{(j,r)} \Omega_{j,s_{in}, \mathbf{F}_{j,s_{in}}}.$$

By modelling the CSI errors as white Gaussian noises, the proposed optimization scheme can optimize the active and passive beamforming design with imperfect CSI. Based on the obtained results, the real communication performance achieved by the proposed optimization scheme can be computed in the case of imperfect CSI.

V. NUMERICAL RESULTS

In this section, we will examine the feasibility and the communication performance for the proposed IRS backscatter based uplink coordinated multi-cell MIMO network by extensive numerical simulations, including the convergence behavior of the optimization schemes, how the element number at IRS, the transmit power budget at the PB, the antenna number of BSs, the cell number and the UE number of each cell affect the achievable WSR of system, and the robustness of the proposed optimization scheme. Besides the proposed optimization scheme, several other benchmark schemes are given for comparison.

- **Joint:** This legend represents the proposed optimization scheme for the considered IRS backscatter based uplink coordinated multi-cell MIMO network, in which FP and alternative optimization are employed to convert the log-

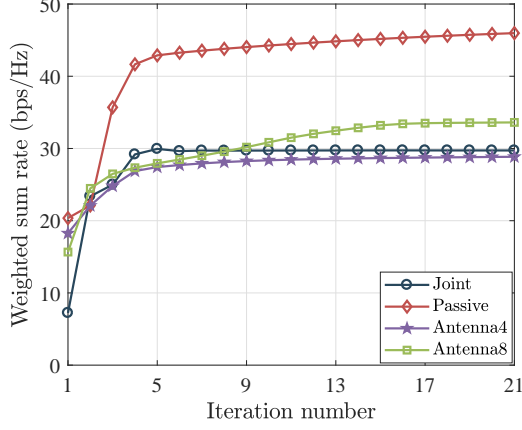


Fig. 3. Convergence behavior of the schemes of Joint, Passive, Antenna4 and Antenna8 for the uplink coordinated multi-cell MIMO network in a random observation.

arithm objective functions into a more tractable form and to handle the coupled optimization variables, as detailed in Section III.

- **Antenna4 and Antenna8:** The two legends denote the optimization schemes for the conventional uplink coordinated multi-cell MIMO network, in which each UE employs active antennas ('4' and '8' denote the antenna number) to communicate with BSs without the deployment of PB.
- **Passive:** This legend represents a specific optimization scheme for the simplified IRS backscatter based uplink coordinated multi-cell MIMO network, in which the PB is removed and the reflection power at each IRS element is equal. For a fair performance comparison between IRS backscatter and active antennas, the reflection power at each IRS in Passive is set to be the same as active antennas in Antenna4 and Antenna8.
- **Discrete4 and Discrete8:** The two legends denote the discrete optimization schemes for the considered IRS backscatter based uplink coordinated multi-cell MIMO network. The only difference of Discrete4 and Discrete8 ('4' and '8' denote the number of discrete values) from Joint is that the passive beamforming at each IRS is discrete.

A. Simulation Setup

In the numerical simulations, we consider Rician fading, with the Rician factor κ , for all involved channels. Let d_x and d_0 denote the transmission distance and the reference distance, respectively. Then, the path loss can be modelled as $PL = PL_0 - 25 \lg(d_x/d_0)$ dB with $PL_0 = -30$ dB. Generally speaking, the incoming signal is only reflected by the front half-sphere of IRS, and thus there exists a 3 dBi gain for the reflection. In Fig. 3, the spatial distribution of PB, BSs and UEs is shown, where the PB is deployed in the ordinate origin (0, 0) while two BSs with the same antenna number are located in the positions (-50, 0) and (50, 0), respectively. For simplicity, the UE number in each cell is identical and the positions of UEs are randomly and independently generated within the radius r of cell. In TABLE I, some important

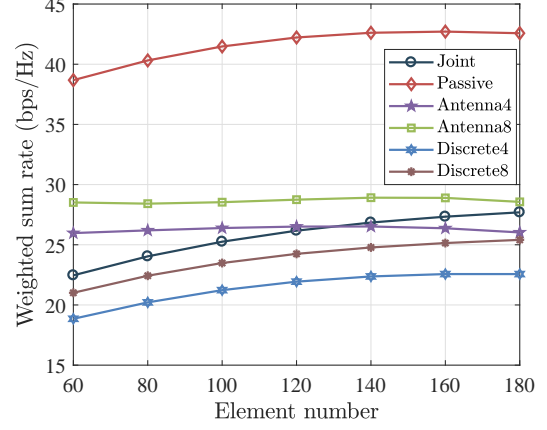


Fig. 4. The relationship between the element number of IRS and the achievable WSR of system for the proposed IRS backscatter based uplink coordinated multi-cell MIMO network.

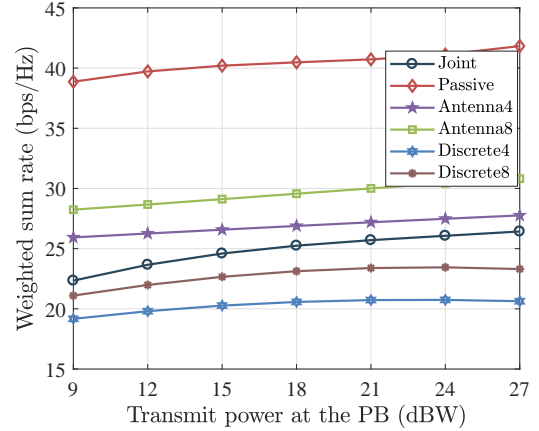


Fig. 5. The relationship between the total transmit power at the PB and the achievable WSR of system for the proposed IRS backscatter based uplink coordinated multi-cell MIMO network. Note that the total transmit power in Passive, Antenna4 and Antenna8 ranges from 3 dBm to 9 dBm, with the step length being 1 dBm.

parameters for the numerical simulations are listed, where some of them may be used as variables in some figures.

B. Convergence Behavior

Fig. 4 shows the convergence behavior of the schemes of Joint, Passive, Antenna4 and Antenna8 for the uplink coordinated multi-cell MIMO network in a random observation. From Fig. 4, it is clearly observed that the schemes of Joint, Passive, Antenna4 and Antenna8 converge very quickly. When the iteration reaches five times, the achievable WSR tends to level off. By comparing Passive with Antenna4 and Antenna8, it can be found that the proposed framework of IRS backscatter gains a better communication performance. That is primarily because the element number of IRS is far more than the active antenna number, which brings a higher degree of spatial freedom.

C. Element Number and Transmit Power vs. WSR

Figs. 5 and 6 depict the impact of the element number of IRS and the total transmit power at the PB on the achievable

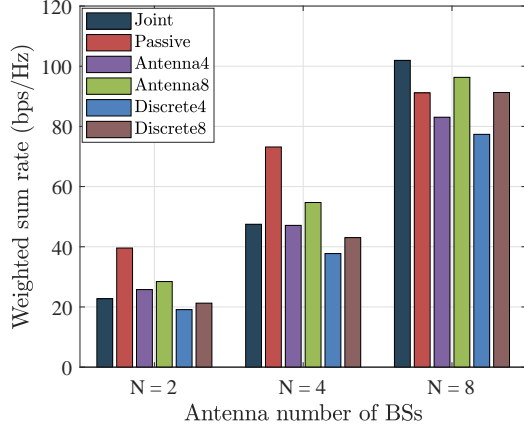


Fig. 6. The relationship between the antenna number of BSs and the achievable WSR of system for the proposed IRS backscatter based uplink coordinated multi-cell MIMO network.

WSR of system for the proposed IRS backscatter based uplink coordinated multi-cell MIMO network, respectively. Note that the total transmit power in Passive, Antenna4 and Antenna8 ranges from 3 dBm to 9 dBm, with the step length being 1 dBm. From Figs. 5 and 6, it can be seen that the achievable WSR of system is improved in the schemes of Joint, Passive, Discrete4 and Discrete8, when the number of elements on each IRS increases or higher total transmit power at the PB is utilized. For the schemes of Antenna4 and Antenna8, an increase in the total transmit power contributes to improving the achievable WSR of system. By comparison, the scheme of Joint is slightly superior to Discrete4 and Discrete8, which indicates that the proposed IRS backscatter scheme can be applied to practical discrete phase and amplitude. On the other hand, the IRS backscatter scheme can be assessed by comparing the schemes of Antenna4 and Antenna8 with Passive. Among all these schemes, Passive achieves the maximum communication performance. Therefore, it can be concluded that a higher degree of spatial freedom owing to many IRS elements is beneficial to facilitating communication performance. It is worth mentioning that the huge energy loss of EM wave from the PB to the IRSs is an adverse factor, observing that Passive, with far lower total power consumption, outperforms Joint. This result implies that the deployment of PB is crucial to the network energy consumption.

D. Antenna, Cell and UE Number vs. WSR

Figs. 6, 7 and 8 depict the impact of the antenna number of BSs, the cell number, and the UE number of each cell on the achievable WSR of system for the proposed IRS backscatter based uplink coordinated multi-cell MIMO network. In the numerical simulations, when the cell number is set as $I = 4$, four BSs are positioned at (50, 0), (-50, 0), (0, 50), and (0, -50), respectively. If I is less than four, any I positions are selected from them to place the BSs. From these simulation figures, it is seen that an increase in the antenna number of BSs, the cell number, and the UE number of each cell can increase the achievable WSR of system. The reasons are summarized as follows: 1) When the BSs are equipped with more antennas,

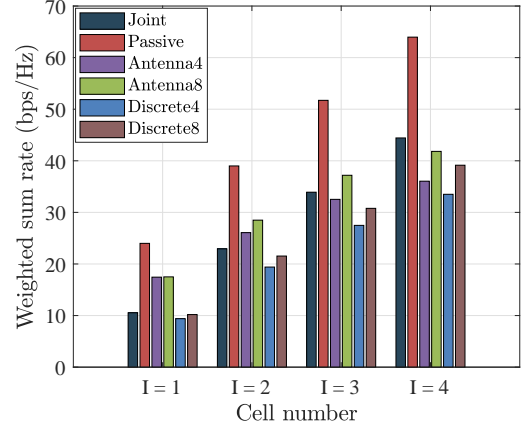


Fig. 7. The relationship between the cell number and the achievable WSR of system for the proposed IRS backscatter based uplink coordinated multi-cell MIMO network.

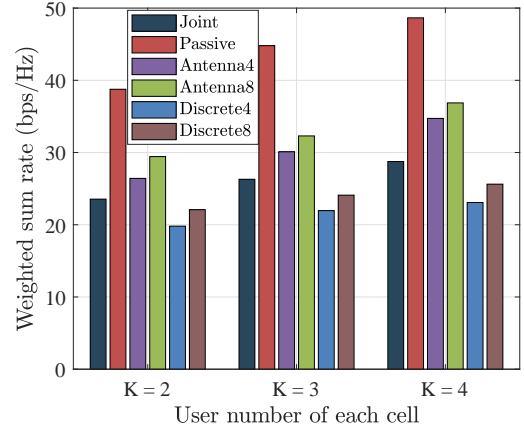


Fig. 8. The relationship between the UE number of each cell and the achievable WSR of system for the proposed IRS backscatter based uplink coordinated multi-cell MIMO network.

more data streams and more cell UEs can be supported for simultaneous uplink transmission in a cell; 2) When more BSs are deployed to form more cells, more energy from the PB can be harvested and more UEs can be scheduled to access wireless network; 3) When more UEs of each cell exist, the degree of spatial freedom is improved. These simulation results further verify that the proposed IRS backscatter based uplink coordinated multi-cell MIMO network is feasible.

E. Robustness of Joint

In wireless communications, it is idealistic to assume that perfect CSI can be acquired. Moreover, IRS enabled communication systems are more susceptible to CSI errors than conventional systems. Taking these factors into consideration, it is necessary to examine the robustness of the proposed optimization scheme of Joint. Fig. 9 shows the impact of channel estimation error on the achievable WSR of system for the proposed IRS backscatter based uplink coordinated multi-cell MIMO network, with three cases including “case 1: $\sigma^2 = -94$ dBm”, “case 2: $\sigma^2 = -85$ dBm”, “case 3: $\sigma^2 = -76$ dBm”. In the numerical simulations, the proposed

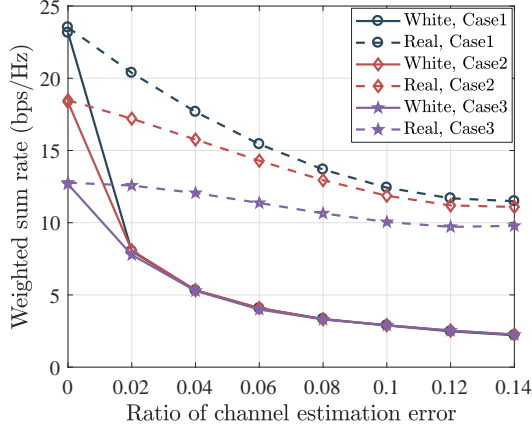


Fig. 9. The impact of channel estimation error on the achievable WSR of system for the proposed IRS backscatter based uplink coordinated multi-cell MIMO network.

optimization scheme is adopted indiscriminately, whose simulation results are denoted by the legend `White`. Based on the obtained active beamforming at the PB, passive beamforming at the IRSs and uplink user scheduling, the real WSR of system can be computed, whose simulation results are denoted by the legend `Real`. From Fig. 9, it can be seen that the curves of `Real` decline slowly, which indicates that the proposed optimization scheme of `Joint` has a good robustness. Additionally, Fig. 9 shows how noise variance affects the achievable WSR of system. When noise variance becomes bigger, the robustness of the proposed scheme of `Joint` gets better. That is because the impact of the components related to the CSI errors becomes weak with noise variance increasing.

VI. CONCLUSIONS

This paper proposed an IRS backscatter based uplink coordinated transmission strategy for a radio cellular network. In this network, we investigated the WSR maximization problem and employed the methods of FP, alternative optimization and weighted bipartite matching to solve it. By simulations, it was verified that an increase in the element number of IRS, the total transmit power at the PB, the antenna number of the BSs, the cell number, and the UE number of each cell contributes to improving the achievable WSR of system. In addition, it was verified that the proposed optimization scheme had a good robustness, especially in the case of large noise variance. On the other hand, like conventional uplink coordinated transmission framework in which the UEs were equipped with active antennas, the proposed paradigm of IRS backscatter achieved a satisfactory WSR of system with consuming the same transmission power. These results confirmed the feasibility of the proposed IRS backscatter based uplink coordinated transmission strategy.

VII. APPENDICES

A. Quadratic Transform

Lemma 1 (Quadratic Transform [13]): Let us consider a typical FP problem as follows.

$$\begin{aligned} \max_{\mathbf{x}} \quad & \frac{A(\mathbf{x})}{B(\mathbf{x})}, \\ \text{s.t.} \quad & \mathbf{x} \in \mathcal{X}, \end{aligned}$$

where \mathcal{X} represents a nonempty set of complex constraint, $A(\mathbf{x})$ is a nonnegative function set, and $B(\mathbf{x})$ represents a positive function set. This problem can be equivalently written as

$$\begin{aligned} \max_{\mathbf{x}, y} \quad & 2y\sqrt{A(\mathbf{x})} - y^2B(\mathbf{x}), \\ \text{s.t.} \quad & \mathbf{x} \in \mathcal{X}, y \in \mathbb{C}. \end{aligned}$$

It is not difficult that quadratic transform also applies to the case of sum-of-functions-of-ratio. To be specific, the problem containing sum-of-functions-of-ratio is expressed as

$$\begin{aligned} \max_{\mathbf{x}} \quad & \sum_{m=1}^M \frac{A_m(\mathbf{x})}{B_m(\mathbf{x})}, \\ \text{s.t.} \quad & \mathbf{x} \in \mathcal{X}. \end{aligned}$$

This problem is equivalent to

$$\begin{aligned} \max_{\mathbf{x}, \mathbf{y}} \quad & \sum_{m=1}^M 2y_m\sqrt{A_m(\mathbf{x})} - y_m^2B_m(\mathbf{x}), \\ \text{s.t.} \quad & \mathbf{x} \in \mathcal{X}, \mathbf{y} \in \mathbb{C}^M, \end{aligned}$$

where \mathbf{y} represents (y_1, y_2, \dots, y_M) .

B. Proof of Proposition 1

According to Section III-A, it can be derived that

$$\begin{aligned} \sum_{(i,n)} \omega_{i,s_{in}} R_{i,s_{in}} &= \sum_{(i,n)} \omega_{i,s_{in}} \log(1 + \gamma_{i,s_{in}}) \\ &= \max_{\alpha_{i,s_{in}} \geq 0} f(\mathbf{w}, \mathcal{V}, \mathcal{S}, \alpha, \beta) \geq f(\mathbf{w}, \mathcal{V}, \mathcal{S}, \alpha, \beta) \end{aligned}$$

During the iteration process, an alternative optimization procedure is employed to address the problem (P1) by cyclically optimizing the variables α , β , \mathbf{w} , \mathcal{V} and \mathcal{S} , which is divided into three steps. In the first step, $\alpha_{i,s_{in}}$ and $\beta_{i,s_{in}}$ are optimized to maximize $f(\mathbf{w}, \mathcal{V}, \mathcal{S}, \alpha, \beta)$ with \mathbf{w} , \mathcal{V} and \mathcal{S} fixed. Therefore, $f(\mathbf{w}, \mathcal{V}, \mathcal{S}, \alpha, \beta)$ is monotonically nondecreasing in this step. Similarly, $f(\mathbf{w}, \mathcal{V}, \mathcal{S}, \alpha, \beta)$ also remains nondecreasing in each of the second step and the third step. After each loop iteration, the objective function $f(\mathbf{w}, \mathcal{V}, \mathcal{S}, \alpha, \beta)$ is monotonically nondecreasing. Note that the rank-one vector solution recovered by Gaussian randomization in Section III-B can achieve a close communication performance to the corresponding matrix solution, which is verified through a lot of observations. In other words, the Gaussian randomization method has little effect on the convergence of the overall algorithm. Mathematically, the alternative optimization procedure is characterized as

$$f(\mathbf{w}^{(t+1)}, \mathcal{V}^{(t+1)}, \mathcal{S}^{(t+1)}, \alpha^{(t+1)}, \beta^{(t+1)})$$

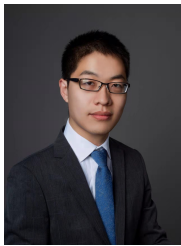
$$\begin{aligned}
&\geq f(\mathbf{w}^{(t+1)}, \mathcal{V}^{(t)}, \mathcal{S}^{(t)}, \alpha^{(t+1)}, \beta^{(t+1)}) \\
&\geq f(\mathbf{w}^{(t)}, \mathcal{V}^{(t)}, \mathcal{S}^{(t)}, \alpha^{(t+1)}, \beta^{(t+1)}) \\
&\geq f(\mathbf{w}^{(t)}, \mathcal{V}^{(t)}, \mathcal{S}^{(t)}, \alpha^{(t)}, \beta^{(t)}).
\end{aligned}$$

Since the value of $f(\mathbf{w}, \mathcal{V}, \mathcal{S}, \alpha, \beta)$ is bounded above, the proposed algorithm must converge. At the convergence, the proposed algorithm can arrive at a local optimum of the formulated optimization problem. Further, for the fixed scheduling variable \mathcal{S} , the solution is a stationary point of the original problem (P1), according to [14].

REFERENCES

- [1] S. Chen, T. Zhao, H. -H. Chen, *et al.*, "Network densification and path-loss models versus UDN performance: A unified approach," *IEEE Trans. Wireless Commun.*, vol. 20, no. 7, pp. 4058-4071, Jul. 2021.
- [2] S. Buzzi, C. I. T. E. Klein, H. V. Poor, *et al.*, "A survey of energy-efficient techniques for 5G networks and challenges ahead," *IEEE J. Sel. Areas Commun.*, vol. 34, no. 4, pp. 697-709, Apr. 2016.
- [3] D. Gesbert, S. Hanly, H. Huang, *et al.*, "Multi-cell MIMO cooperative networks: A new look at interference," *IEEE J. Sel. Areas Commun.*, vol. 28, no. 9, pp. 1380-1408, Dec. 2010.
- [4] M. Hua, Q. Wu, D. W. K. Ng, *et al.*, "Intelligent reflecting surface-aided joint processing coordinated multipoint transmission," *IEEE Trans. Commun.*, vol. 69, no. 3, pp. 1650-1665, Mar. 2021.
- [5] R. Zhang, "Cooperative multi-cell block diagonalization with per-base-station power constraints," *IEEE J. Sel. Areas Commun.*, vol. 28, no. 9, pp. 1435-1445, Dec. 2010.
- [6] S. Xu, J. Liu, T. K. Rodrigues, *et al.*, "Envisioning intelligent reflecting surface empowered space-air-ground integrated network," *IEEE Netw.*, vol. 35, no. 6, pp. 225-232, Nov/Dec. 2021.
- [7] S. Xu, J. Liu, Y. Cao, J. Li, *et al.*, "Intelligent reflecting surface enabled secure cooperative transmission for satellite-terrestrial integrated networks," *IEEE Trans. Veh. Technol.*, vol. 70, no. 2, pp. 2007-2011, Feb. 2021.
- [8] Q. Wu, and R. Zhang, "Towards smart and reconfigurable environment: Intelligent reflecting surface aided wireless network," *IEEE Commun. Mag.*, vol. 58, no. 1, pp. 106-112, Jan. 2020.
- [9] M. Di Renzo, A. Zappone, M. Debbah, *et al.*, "Smart radio environments empowered by reconfigurable intelligent surfaces: How it works, state of research, and the road ahead," *IEEE J. Sel. Areas Commun.*, vol. 38, no. 11, pp. 2450-2525, Nov. 2020.
- [10] C. Huang, S. Hu, G. C. Alexandropoulos, *et al.*, "Holographic MIMO surfaces for 6G wireless networks: Opportunities, challenges, and trends," *IEEE Wireless Commun.*, vol. 27, no. 5, pp. 118-125, Oct. 2020.
- [11] S. Hu, F. Rusek, and O. Edfors, "Beyond massive MIMO: The potential of data transmission with large intelligent surfaces," *IEEE Trans. Signal Process.*, vol. 66, no. 10, pp. 2746-2758, May 2018.
- [12] S. Xu, Y. Du, J. Liu, *et al.*, "Weighted sum rate maximization in IRS-BackCom enabled downlink multi-cell MISO network," *IEEE Commun. Lett.*, vol. 26, no. 3, pp. 642-646, Mar. 2022.
- [13] K. Shen, and W. Yu, "Fractional programming for communication systems – Part I: power control and beamforming," *IEEE Trans. Signal Process.*, vol. 66, no. 10, pp. 2616-2630, May, 2018.
- [14] K. Shen, and W. Yu, "Fractional programming for communication systems – Part II: uplink scheduling via matching," *IEEE Trans. Signal Process.*, vol. 66, no. 10, pp. 2631-2644, May15, 2018.
- [15] J. Choi, N. Lee, S. Hong, *et al.*, "Joint user selection, power allocation, and precoding design with imperfect CSIT for multi-cell MU-MIMO downlink systems," *IEEE Trans. Wireless Commun.*, vol. 19, no. 1, pp. 162-176, Jan. 2020.
- [16] Y. Wu, C. Wen, W. Chen, *et al.*, "Data-aided secure massive MIMO transmission under the pilot contamination attack," *IEEE Trans. Commun.*, vol. 67, no. 7, pp. 4765-4781, Jul. 2019.
- [17] C. Huang, R. Mo, and C. Yuen, "Reconfigurable intelligent surface assisted multiuser MISO systems exploiting deep reinforcement learning," *IEEE J. Sel. Areas Commun.*, vol. 38, no. 8, pp. 1839-1850, Aug. 2020.
- [18] C. Huang, Z. Yang, G. C. Alexandropoulos, *et al.*, "Multi-hop RIS-empowered terahertz communications: A DRL-based hybrid beamforming design," *IEEE J. Sel. Areas Commun.*, vol. 39, no. 6, pp. 1663-1677, Jun. 2021.
- [19] H. Yang, Z. Xiong, J. Zhao, *et al.*, "Deep reinforcement learning-based intelligent reflecting surface for secure wireless communications," *IEEE Trans. Wireless Commun.*, vol. 20, no. 1, pp. 375-388, Jan. 2021.
- [20] H. Yang, Z. Xiong, J. Zhao, *et al.*, "Intelligent reflecting surface assisted anti-jamming communications: A fast reinforcement learning approach," *IEEE Trans. Wireless Commun.*, vol. 20, no. 3, pp. 1963-1974, Mar. 2021.
- [21] E. Balevi, A. Doshi, and J. G. Andrews, "Massive MIMO channel estimation with an untrained deep neural network," *IEEE Trans. Wireless Commun.*, vol. 19, no. 3, pp. 2079-2090, Mar. 2020.
- [22] A. A. Khan, and R. S. Adve, "Centralized and distributed deep reinforcement learning methods for downlink sum-rate optimization," *IEEE Trans. Wireless Commun.*, vol. 19, no. 12, pp. 8410-8426, Dec. 2020.
- [23] J. Qiu, J. Yu, A. Dong, *et al.*, "Joint beamforming for IRS-aided multi-cell MISO system: sum rate maximization and SINR balancing," *IEEE Trans. Wireless Commun.*, to be published, doi: 10.1109/TWC.2022.3159564.
- [24] H. Xie, J. Xu and Y. -F. Liu, "Max-min fairness in IRS-aided multi-cell MISO systems with joint transmit and reflective beamforming," *IEEE Trans. Wireless Commun.*, vol. 20, no. 2, pp. 1379-1393, Feb. 2021.
- [25] C. Pan, H. Ren, K. Wang, *et al.*, "Multicell MIMO communications relying on intelligent reflecting surfaces," *IEEE Trans. Wireless Commun.*, vol. 19, no. 8, pp. 5218-5233, Aug. 2020.
- [26] W. Ni, X. Liu, Y. Liu, *et al.*, "Resource allocation for multi-cell IRS-aided NOMA networks," *IEEE Trans. Wireless Commun.*, vol. 20, no. 7, pp. 4253-4268, Jul. 2021.
- [27] Y. Zhang, B. Di, H. Zhang, *et al.*, "Meta-wall: Intelligent omni-surfaces aided multi-cell MIMO communications," *IEEE Trans. Wireless Commun.*, to be published, doi: 10.1109/TWC.2022.3154041.
- [28] W. U. Khan, J. Liu, F. Jameel, *et al.*, "Secure backscatter communications in multi-cell NOMA networks: enabling link security for massive IoT networks," in *Proc. IEEE Conf. Comput. Commun. Workshops (INFOCOM WKSHPS)*, 2020, pp. 213-218.
- [29] P. N. Alevizos, and A. Bletsas, "Inference-based resource allocation for multi-cell backscatter sensor networks," in *Proc. IEEE International Conference on Communications (ICC)*, 2019, pp. 1-6.
- [30] Y. -C. Liang, Q. Zhang, J. Wang, *et al.*, "Backscatter communication assisted by reconfigurable intelligent surfaces," *Proc. IEEE*, to be published, doi: 10.1109/JPROC.2022.3169622.
- [31] W. Tang, J. Dai, M. Chen, *et al.*, "Programmable metasurface-based RF chain-free 8PSK wireless transmitter," *Electron. Lett.*, vol. 55, no. 7, pp. 417-420, Apr. 2019.
- [32] W. Tang, J. Dai, M. Chen, *et al.*, "MIMO transmission through reconfigurable intelligent surface: system design, analysis, and implementation," *IEEE J. Sel. Areas Commun.*, vol. 38, no. 11, pp. 2683-2699, Nov. 2020.
- [33] J. Y. Dai, J. Dai, W. Tang, *et al.*, "Realization of multi-modulation schemes for wireless communication by time-domain digital coding metasurface," *IEEE Trans. Antennas Propag.*, vol. 68, no. 3, pp. 1618-1627, Mar. 2020.
- [34] M. Jung, W. Saad, M. Debbah, *et al.*, "On the optimality of reconfigurable intelligent surfaces (RISs): passive beamforming, modulation, and resource allocation," *IEEE Trans. Wireless Commun.*, vol. 20, no. 7, pp. 4347-4363, Jul. 2021.
- [35] W. Zhao, G. Wang, S. Atapattu, *et al.*, "Is backscatter link stronger than direct link in reconfigurable intelligent surface-assisted system?" *IEEE Commun. Lett.*, vol. 24, no. 6, pp. 1342-1346, Jun. 2020.
- [36] X. Guan, Q. Wu, and R. Zhang, "Joint power control and passive beamforming in IRS-assisted spectrum sharing," *IEEE Commun. Lett.*, vol. 24, no. 7, pp. 1553-1557, Jul. 2020.
- [37] S. Xu, Y. Du, J. Liu, *et al.*, "Intelligent reflecting surface based backscatter communication for data offloading," *IEEE Trans. Wireless Commun.*, to be published, doi: 10.1109/TCOMM.2022.3170629.
- [38] S. Xu, J. Liu, and J. Zhang, "Resisting undesired signal through IRS-based backscatter communication system," *IEEE Commun. Lett.*, vol. 25, no. 8, pp. 2743-2747, Aug. 2021.
- [39] S. Xu, J. Liu, and Y. Cao, "Intelligent reflecting surface empowered physical layer security: signal cancellation or jamming?," *IEEE Internet Things J.*, vol. 9, no. 2, pp. 1265-1275, Jan. 2022.
- [40] L. Wei, C. Huang, Qinghua Guo, *et al.*, "Joint channel estimation and signal recovery for RIS-empowered multiuser communications," *IEEE Trans. Commun.*, vol. 70, no. 7, pp. 4640-4655, Jul. 2022.
- [41] L. Wei, C. Huang, G. C. Alexandropoulos, *et al.*, "Channel estimation for RIS-empowered multi-user MISO wireless communications," *IEEE Trans. Commun.*, vol. 69, no. 6, pp. 4144-4157, Jun. 2021.
- [42] X. Yu, V. Jamali, D. Xu, *et al.*, "Smart and reconfigurable wireless communications: From IRS modeling to algorithm design," *IEEE Wireless Commun.*, vol. 28, no. 6, pp. 118-125, Dec. 2021.

- [43] Q. Wu, and R. Zhang, "Beamforming optimization for wireless network aided by intelligent reflecting surface with discrete phase shifts," *IEEE Trans. Commun.*, vol. 68, no. 3, pp. 1838-1851, Mar. 2020.
- [44] V. Jamali, M. Najafi, R. Schober, *et al.*, "Power efficiency, overhead, and complexity tradeoff of IRS codebook design-quadratic phase-shift profile," *IEEE Communi. Lett.*, vol. 25, no. 6, pp. 2048-2052, Jun. 2021.
- [45] M. Najafi, V. Jamali, R. Schober, *et al.*, "Physics-based modeling and scalable optimization of large intelligent reflecting surfaces," *IEEE Trans. Commun.*, vol. 69, no. 4, pp. 2673-2691, Apr. 2021.
- [46] S. Hu, Z. Wei, Y. Cai, *et al.*, "Robust and secure sum-rate maximization for multiuser MISO downlink systems with self-sustainable IRS," *IEEE Trans. Commun.*, vol. 69, no. 10, pp. 7032-7049, Oct. 2021.



Sai Xu (Member, IEEE) received the B.S. degree from Hebei Normal University, Shijiazhuang, China, in 2012, and the M.E. and Ph.D. degrees from the Harbin Institute of Technology (HIT), Harbin, China, in 2015 and 2020, respectively. He was also a joint Ph.D. student with the Electrical Engineering Department, University of California, Los Angeles, CA, USA, from October 2017 to April 2019. He is currently a Marie Curie Research Fellow with the Department of Electronic and Electrical Engineering, The University of Sheffield. His research

interests include but are not limited to intelligent reflecting surface, backscatter communications, IoT and 5G/6G communications.



Chen Chen (Member, IEEE) received the B.E. degree from the East China University of Science and Technology, in 2018, and the Ph.D. degree from The University of Sheffield, in 2022. Since January 2022, he has been a Postdoctoral Research Associate at the University of Liverpool. His current research interests include massive MIMO, mmWave/THz networks, wireless security, stochastic geometry, optimisation, and machine learning.



Yanan Du (Member, IEEE) received the B.S. degree from Hebei Normal University, Shijiazhuang, China, in 2012, the M.S. degree from South China Normal University, Guangzhou, China, in 2015, and the Ph.D. degree from Harbin Engineering University, Harbin, China, in 2022. She was a Joint Ph.D. Student with the Electrical Engineering Department, University of California, Los Angeles, CA, USA, from October 2017 to April 2019. Since July 2022, she has been a Postdoctoral Fellow at the Northwestern Polytechnical University. Her research interests

include integrated sensing and communication (ISAC), intelligent reflecting surface (IRS), cyber-physical system (CPS), and physical layer security (PLS).



Jiangzhou Wang (Fellow, IEEE) is a Professor with the University of Kent, U.K. He has published more than 400 papers and four books. His research focuses on mobile communications. He was a recipient of the 2022 IEEE Communications Society Leonard G. Abraham Prize and IEEE Globecom2012 Best Paper Award. He was the Technical Program Chair of the 2019 IEEE International Conference on Communications (ICC2019), Shanghai, Executive Chair of the IEEE ICC2015, London, and Technical Program Chair of the IEEE WCNC2013. He is/was the editor of a number of international journals, including IEEE Transactions on Communications from 1998 to 2013. Professor Wang is a Fellow of the Royal Academy of Engineering, U.K., Fellow of the IEEE, and Fellow of the IET.



Jie Zhang (Senior Member, IEEE) received a Ph.D. degree from East China University of Science and Technology, Shanghai, China, in 1995. He has held the Chair in Wireless Systems (on a part-time basis) with the Department of Electronic and Electrical Engineering, University of Sheffield, Sheffield, U.K., since January 2011. He is also the Founder, a Board Director and the Chief Scientific Officer of Ranplan Wireless, Cambridge, U.K., a public company listed on Nasdaq First North. Ranplan Wireless produces a suite of world leading indoor and the first joint

indoor-outdoor radio access network planning tool – Ranplan Professional, which is being used by the worlds largest mobile operators and network vendors across the globe. Along with his students and colleagues, he has pioneered research in small cell and heterogeneous network and published some of the landmark papers and book on these topics, widely used by both academia and industry. Since 2010, he and his team have also developed ground-breaking work in building wireless performance modelling, evaluation and optimization, the key concepts of which were introduced in Fundamental Wireless Performance of a Building, IEEE Wireless Communications, 29(1), 2022. His Google scholar citations are in excess of 8000 with an H-index of 39.